

Corrosion behaviour of TaN thin PVD films on steels

J. F. Flores*¹, J. J. Olaya², R. Colás¹, S. E. Rodil³, B. S. Valdez⁴ and I. G. Fuente⁵

The corrosion behaviour of tantalum nitride (TaN) thin films deposited on AISI 1018 carbon steel, AISI M2 tool steel and AISI 304 stainless steel has been investigated in an aqueous sodium chloride solution. The films were produced by means of magnetron sputtering plasma deposition. Morphological and microstructural characteristics of the films were studied by atomic force microscopy and X-ray diffraction analysis. Potentiodynamic polarisation, electrochemical impedance spectroscopy and cyclic voltammetry techniques were used for electrochemical characterisation. The TaN films displayed lower corrosion current densities than those of the substrates. A relaxation time in the impedance analysis was observed in the 1018/TaN system, two relaxation times were observed in the M2/TaN system, and a diffusion process was found in the 304/TaN system. This indicates that the substrates were not completely isolated from the solution and the defects in the films appear to be detrimental owing to electrolyte penetration through the defects which caused localised corrosion. The corrosion behaviour of the films depends mainly on the electrochemical properties of the substrate.

Keywords: Tantalum nitride, Corrosion, Electrochemical impedance spectroscopy, Cyclic voltammetry, Potentiodynamic polarisation, Surface analysis, Magnetron sputtering

Introduction

Most of the engineering materials used in industry have to be protected against corrosion using surface techniques. Physical vapour deposition (PVD) coating is a widely used technique to enhance the surface properties of engineering alloys. PVD coatings based on nitrides, carbides or a combination of the two increase significantly the lifetime and service quality of different substrates owing to reduced friction and better thermal and corrosion stability in aggressive environments.¹⁻⁴ TaN thin films have been utilised as structural elements in integrated circuits.⁵⁻⁷ Most of the work performed on TaN has been related to its application in thin film resistors and diffusion barriers for aluminium and silicon. Thin films have been used extensively as the key elements of mask absorbers for X-ray lithography and the magnetic multilayers of recording heads.^{8,9} Relatively little work has been carried out on their application as hard wear resistant coatings or for corrosion protection. There have, however, been studies

of their corrosion performance in alkali media and in an acidic electrolyte. In both media, cyclic voltammetry (CV) was applied for the electrochemical characterisation.¹⁰⁻¹³ PVD coatings generally exhibit growth defects such as pores and pinholes, through which corrosion attack of the substrate takes place.^{14,15}

The present study has focused on the effect exerted by the substrate on the corrosion activity of TaN thin films through their electrochemical characterisation in a chloride medium. Potentiodynamic polarisation, CV and electrochemical impedance spectroscopy (EIS) were used for the electrochemical characterisation. Scanning electron microscopy (SEM) and atomic force microscopy (AFM) were applied for the surface characterisation of the corroded systems.

Experimental procedure

Three different steels were selected as the substrates for the present work: a structural carbon steel (CS) AISI 1018, a tool steel (TS) AISI M2 and a stainless steel (SS) AISI 304. Table 1 presents the chemical compositions of these materials, which comply with the specifications

¹Facultad de Ingeniería Mecánica y Eléctrica, Universidad Autónoma de Nuevo León, San Nicolás de los Garza, NL, México

²Unidad de materiales, Dpto. de Ingeniería Mecánica y Mecatrónica, Universidad Nacional de Colombia, ciudad Universitaria, Bogotá Colombia

³Instituto de Investigaciones en Materiales, Universidad Nacional Autónoma de México, México DF, México

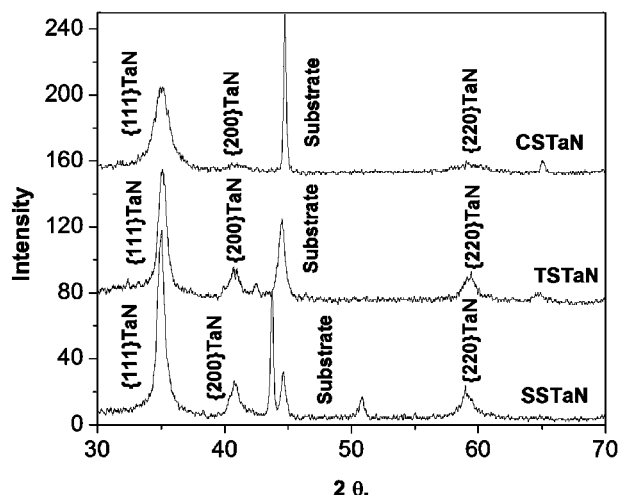
⁴Instituto de Ingeniería, Laboratorio de Corrosión y Materiales Red Nacional de Corrosión, Universidad Autónoma de Baja California, Mexicali, Baja California, México

⁵Facultad Ciencias Químicas, Universidad Autónoma de Nuevo León, San Nicolás de los Garza, NL, México

*Corresponding author, email jff11@pitt.edu

Table 1 Chemical composition of substrates, wt-%

Steel	Element								
	UNS	C	Si	Mn	Cr	Ni	Mo	W	V
1018	G10180	0.18	0.20	0.75					
M2	T11302	0.85			4.2		5.0	6.2	1.85
304	S30400	0.08	1.0	2.0	19.0	9.0			



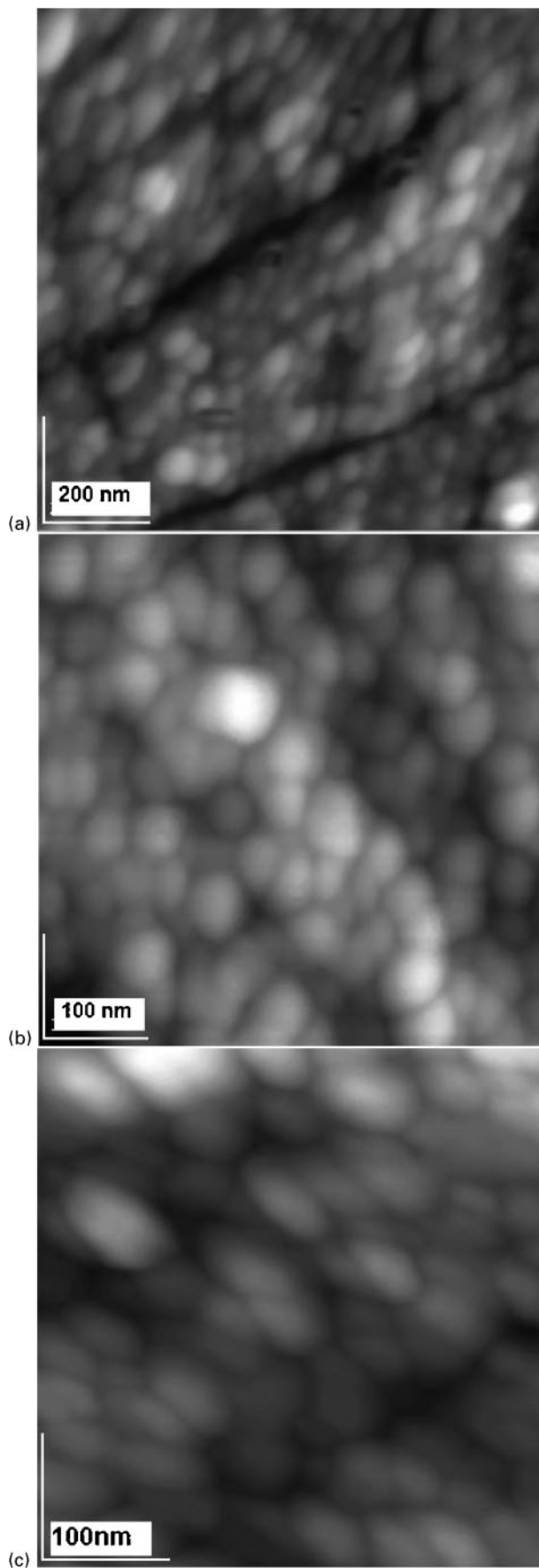
1 X-ray diffraction patterns of coated steels

given by the American Iron and Steel Institute (AISI).¹⁶ The carbon and tool steel were obtained as rods machined down to 10 mm in diameter, whereas the stainless steel was obtained as a thin strip cut into 10 mm² pieces.

The substrate samples were ground with successively finer grades of silicon carbide paper, and finally polished to a 1 μm diamond finish. They were cleaned in an ultrasonic bath with acetone and ethanol for 5 min and dried with hot air.

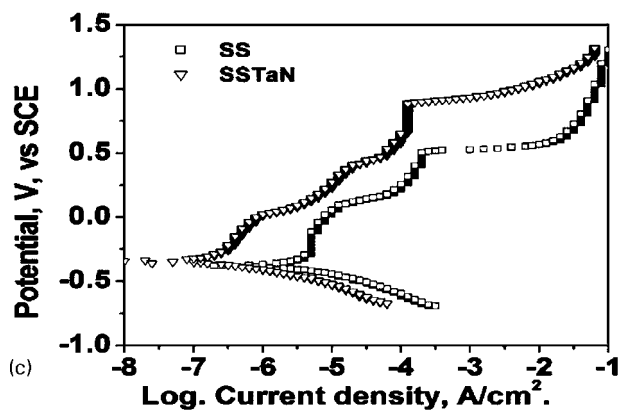
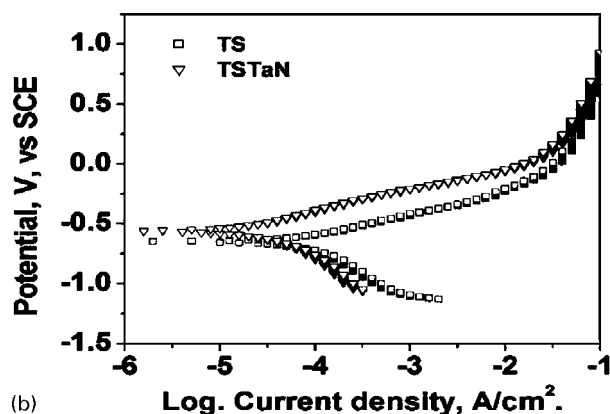
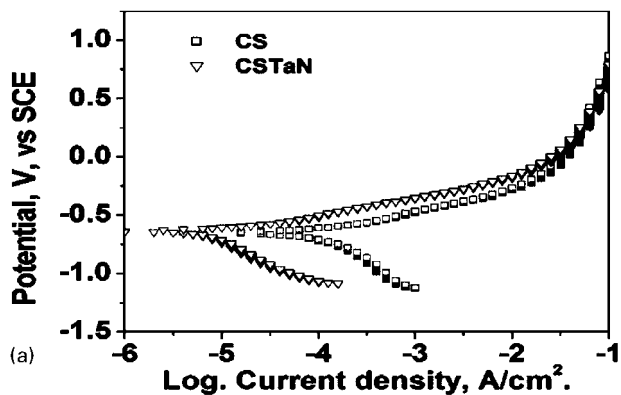
The TaN films were deposited by magnetron sputtering; care was taken to keep the temperature below 200°C, using 14 cm³ min⁻¹ of argon as the plasma gas and 2 cm³ min⁻¹ of nitrogen as the reactive gas, and a deposition pressure of 1.2 Pa. A tantalum target was used for the deposition. The crystallographic structures of the films were studied by X-ray diffraction (XRD) using Cu K_α radiation. The diffraction intensity was recorded over a range of scattering angles of 30–120°. The surface morphology of the films was investigated with AFM in non-contact mode using a silicon nitride cantilever. For the corrosion tests a conventional three electrode cell was arranged with a counter electrode and a saturated calomel electrode (SCE) as the reference electrode. The electrochemical experiments were performed in a 3% NaCl solution at room temperature; the working electrode area was 0.254 cm². The scanning rate in the potentiodynamic polarisation tests, which were conducted after the sample had been immersed in the solution for 2 h, was 5 mV s⁻¹, and the potential range used went from -0.5 V_{SCE} to 1.5 V_{SCE}. EIS measurements for coated and uncoated samples were collected as a function of exposure time at intervals of 1, 24, 48 and 72 h; a perturbation ac potential of 10 mV in amplitude was applied over a frequency range 10⁻²–10⁴ Hz; a data density of ten frequency points per decade was used. The impedance spectra were analysed by equivalent circuits using the Gamry Echem analyst software to determine the characteristic electrochemical parameters.

CV tests were carried out at a potential scanning rate of 15 mV s⁻¹ in order to get smooth curves; using a scanning rate of 5 mV s⁻¹ gave rise to noisy curves. The voltage scanning range for the SS/TaN system was -1.5 V_{SCE}–0.8 V_{SCE}, for the CS/TaN system it was -1.0 V_{SCE}–0.6 V_{SCE} and for the TS/TaN system it was -1.0 V_{SCE}–0.5 V_{SCE}. The samples were examined by SEM and AFM before and after the corrosion test.



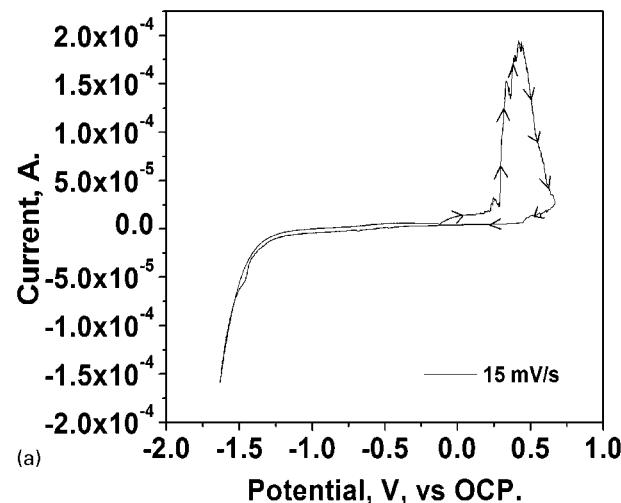
a CS/TaN; b TS/TaN; c SS/TaN

2 AFM images of TaN film surface



a CS and CS/TaN systems; b TS and TS/TaN systems; c SS and SS/TaN systems

3 Polarisation scans of TaN coated steels in 3%NaCl solution after 2 h of immersion



Results and discussion

The structure of the TaN films was studied as a function of the substrate by XRD. Figure 1 shows X-ray spectra of the films, consisting exclusively of the face centred cubic TaN phase; the diffraction planes were {111}, {200} and {220}. No differences were noticed in the film structure related to the substrate. Similar results have been reported in other publications.⁵⁻¹⁰ The surface morphology was investigated using AFM. The films displayed a very fine granular structure with a rounded shape (Fig. 2a-c); no significant changes of the films related to the substrate were detected.

The polarisation plots of the TaN films in 3%NaCl solution indicated that all samples had higher corrosion potential and better corrosion resistance than the bare substrates (Fig. 3a-c). The electrochemical parameters are listed in Table 2; for the uncoated carbon steel the current density i_{corr} was $20 \mu A cm^{-2}$. This was at least fifteen times higher than that of the coated samples. In the case of the tool steel, the current density was seven times higher for uncoated steel than for coated steel. For the stainless steel, the current density for uncoated material was four times that for coated material.

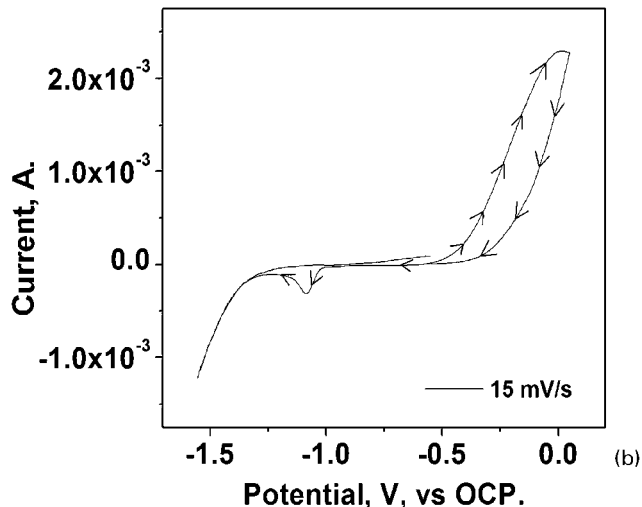
The corrosion current density is an important parameter to evaluate the kinetics of corrosion reactions. Corrosion protection¹⁷ is normally proportional to the corrosion current density measured via polarisation (Fig. 3, Table 2a).

Ideally, a coating such as Ta deposited without impurities or defects would exhibit the same corrosion behaviour as its bulk metal, because there is no change in its chemical nature. However, in practice it is generally not feasible to achieve such coatings, especially thin ones.¹⁸

The TaN is chemically inert and hence, the polarisation resistance of TaN films measured at open circuit potential is represented by the resistance of the substrate exposed to the electrolyte through open pores. Determination of porosity is difficult because of the small size of the defects.¹⁵ The porosity of active materials can be estimated by equation (1)¹⁹

$$P = [R_{ps(substrate)} / R_{pc(system)}] 10^{-(|\Delta E_{corr}| / \beta a)} \quad (1)$$

Where P is the estimated porosity of the film, R_{ps} and R_{pc} are the polarisation resistance of the bare substrate



a SS/TaN; b CS/TaN

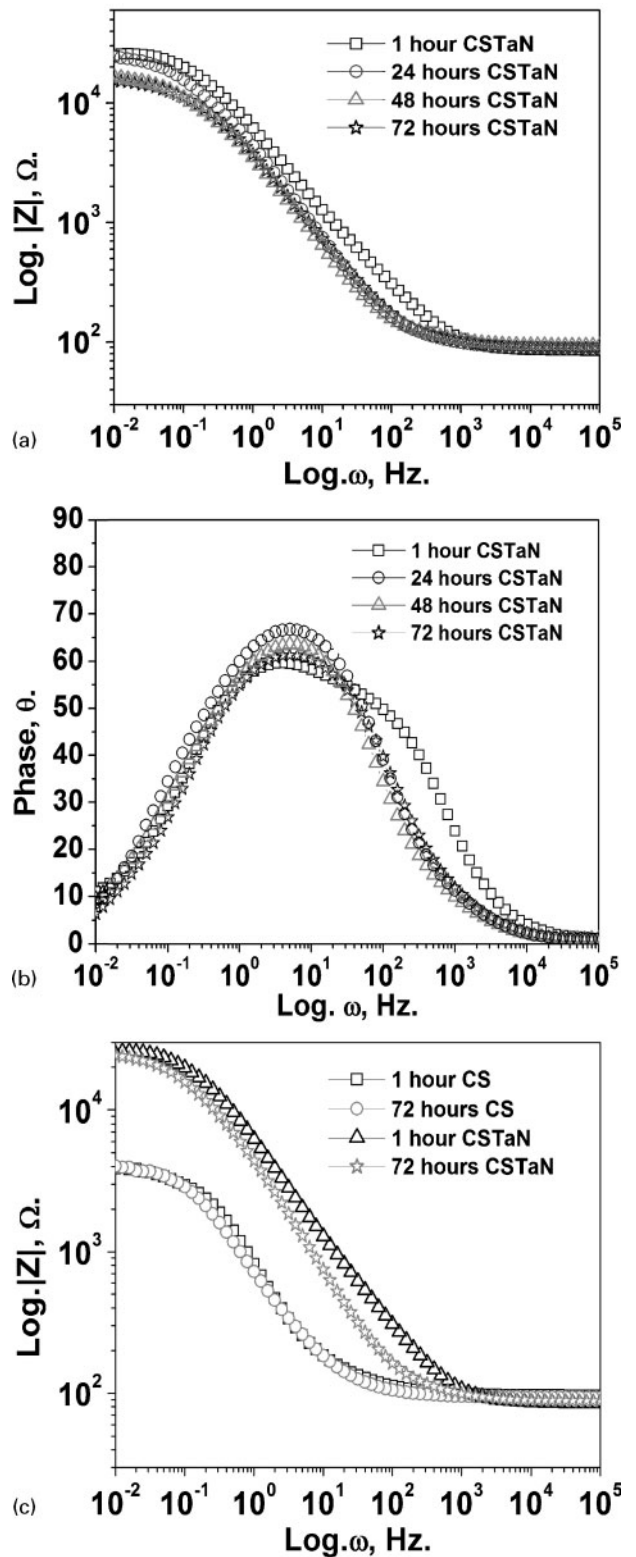
4 Cyclic voltammograms for TaN coated steels after 2 h of immersion in 3%NaCl

and the film respectively, ΔE_{corr} is the difference of corrosion potential between the coating and the base metal and βa is the anodic Tafel slope for the substrate.¹⁹ For the polarisation plots of the CS/TaN and TS/TaN systems, the coated steel reproduced some features of the substrate shape. The SS/TaN system was the only one that displayed passive behaviour.

Cyclic voltammetry has been used previously in the electrochemical characterisation of thin films^{20,21} to obtain information about the double layer capacitance (the dielectric characteristic of the film), the electrochemical window (the potential range within which cations and anions are inert toward electrochemical oxidation and reduction), the surface activity (i.e. the ability to form protective layers) and porosity.^{22,23} The voltammograms obtained for the systems SS/TaN and CS/TaN are shown in Fig. 4a and b respectively. There are significant differences in the electrochemical behaviour of the samples under investigation. On the positive forward scan for the SS/TaN system (Fig. 4a) three oxidation peaks were mainly observed. These peaks show that more oxidation products were formed. The oxidation potential range was small (0.439–0.421 V) and also the reverse scan of the sweep showed no cathodic peaks, indicating the formation of electrochemically inactive products. The electrochemical window was observed in the range -1.13 – 0.439 V. Figure 4b depicts the cyclic voltammogram obtained for the CS/TaN system. The electrochemical potential window was observed in the range -1.0 – 0.567 V. The cyclic voltammogram showed one oxidation peak at 0.018 V with 2.29 mA; the peak width²⁴ indicates the presence of an autocatalytic process that involved dissolution and fracture of the corrosion products formed on the sample surface. The presence of chloride ions in the solution contributed to the formation of pits on the film surface. The sample showed a cathode peak at -1.08 V and a passivation process was not observed.

EIS is a very effective technique that helps in the analysis of various steps involved in an electrochemical reaction by measuring the impedance system response to small ac potential signals over a wide frequency range.²⁵ Information about the coating/solution interface and substrate/solution interface may be obtained by this technique.¹⁷ Over a frequency bandwidth of interest, the impedance spectrum can be presented in various ways: in the Nyquist format that the impedance values at each frequency are resolved into the real and imaginary terms, in the Bode plot, with the impedance modulus data $|Z|$ associated with resistive and capacitive elements, and in the phase plot, which is associated with the dielectric properties of the film.^{26,27}

The Bode plot (Fig. 5a) shows the behaviour of the CS/TaN system after immersion for different times from 1 to 72 h; resistive behaviour was identified at high and low frequencies, which is encountered typically in a

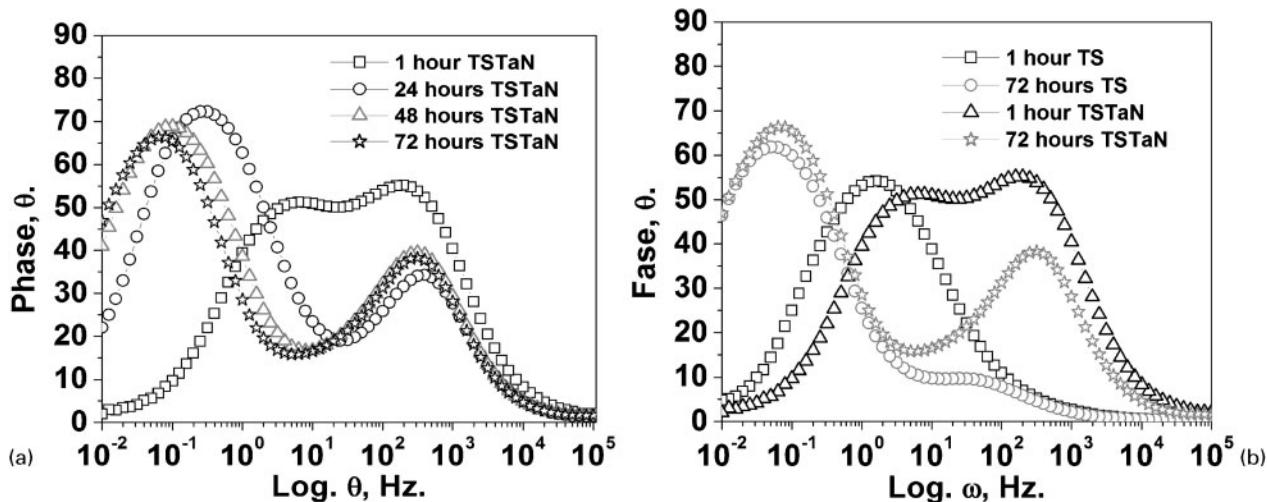


a Bode plot for CS/TaN; b phase representation for CS/TaN; c Bode

5 Impedance spectra comparison of impedance response between uncoated and coated carbon steels

Table 2 Electrochemical polarisation parameters in 3%NaCl solution after 2 h of immersion time

Specimen	E (OCP), mV	i_{corr} , $\mu\text{A cm}^{-2}$	R_p , $\text{k}\Omega \text{ cm}^2$	Porosity, P
CS	628	20	0.34	NA
CS/TaN	591	1.34	35.1	0.0064
TS	630	17.1	0.36	NA
TS/TaN	562	2.25	1.8	0.0954
SS	192	0.683	53.3	NA
SS/TaN	177	0.177	232.5	NA



a phase representation of TS/TaN system; b phase
 6 Impedance spectra comparison of impedance response between uncoated and coated tool steel

charge transfer process. The phase angle (Fig. 5b) diminished as the immersion time increased; this indicates penetration of the electrolyte through defects in the film such as pores, pinholes, droplets and cracks. The Bode spectra of uncoated and coated samples are compared in Fig. 5c; the $|Z|$ values for the coated steel were approximately one order of magnitude higher than in the case of coated samples, which demonstrates the better corrosion performance of the coated steel.

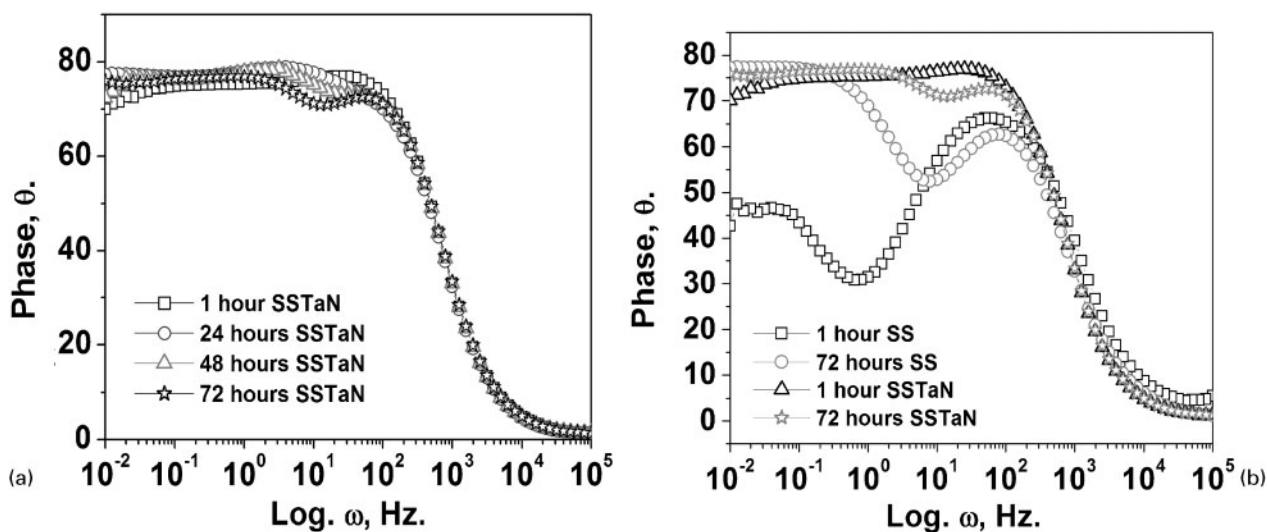
For the TS/TaN system, the phase angle spectra (Fig. 6a) show two relaxation times which are better resolved at longer exposure times. The high frequency relaxation process is attributed to the coating/solution interface and represents the dielectric properties of PVD coatings, whereas the low frequency process is associated with the substrate/solution interface and represents the corrosion process of the substrate in the pores.^{16,28} As the immersion time increases, the peak height decreases, which indicates that the film response became less capacitive.

The phase spectra for uncoated and TaN coated tool steel are presented in Fig. 6b. The coated sample shows better dielectric properties at higher values of ω and θ .

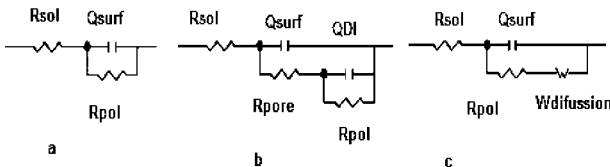
After 1 h of immersion time the TS did not show evidence of a protective film but, as the time increased, two time constants were observed, the phase angle values for the coated sample being higher than those for the uncoated sample.

For the SS/TaN system the phase spectra after various immersion times are presented in Fig. 7a. The phase angles were close to 90°, representing a pure capacitive response throughout the 72 h of exposure. It is expected that the response from the SS at pores is also capacitive as it is highly passive. The passive layer is normally an inert thin film with a low conductivity, which results in a capacitive response similar to that from PVD ceramic coatings, so that only a single time constant is observed.²⁹ A comparative examination (Fig. 7b) demonstrated the better electrochemical and corrosion behaviour of the coated sample. Evidence of two time constants was observed for the phase spectra in the SS analysis; these indicated minor capacitive and dielectric properties for the passive films on the stainless steel.

EIS modelling is usually carried out using an equivalent circuit (EC), which is an assembly of circuit elements representing the physical and electrical features



a phase representation of SS/TaN system; b phase
 7 Impedance spectra comparison of impedance response between uncoated and coated stainless steel



a charge transfer process; b two time constant process; c diffusion process

8 Equivalent circuits for corrosion behaviour of electrochemical system used in simulation of EIS spectra

of the electrochemical interface. Figure 8a–c shows the equivalent circuits for the systems studied. In Fig. 8a the circuit represents charge transfer behaviour for the CS and the CS/TaN systems. As could be seen in Fig. 5a–c for the CS/TaN system, a second relaxation time was not evident. This is attributed to the fact that the TaN film was not compact and thick enough to avoid the penetration of electrolyte through the film. The electrolyte immediately penetrates the open pores and reaches the steel, so that R_{pore} is almost negligible. The failure mode and the EDAX analysis of the corroded samples will be presented later. R_{sol} is the solution resistance between the working electrode and reference electrode, R_{pol} is the resistance of the surface and Q_{surf} is the capacitance of the surface.

The capacitance was replaced by a constant phase element (CPE). The impedance of the CPE is given by equation (2)

$$Z_{CPE} = Z_O(j\omega)^{-n} \tag{2}$$

where Z_O is the adjustable parameter used in the non-linear least squares fitting and the factor n is defined as a CPE exponent that always lies between 0.5 and 1. It can be obtained from the slope of $|Z|$ and the Bode plot. When $n=0.5$ the CPE represents a Warburg impedance with a diffusional character.²⁸ Figure 8b shows the equivalent circuit representing the behaviour with two time constants, which presents R_{pore} and Q_{surf} , the elements describing the electrochemical characteristics of the oxide layer on the surface. Figure 8c shows the equivalent circuit for the SS/TaN system; the diffusion of reactive species is important and always exists in electrochemical corrosion. The Warburg impedance is usually employed to model semi-infinite diffusion behaviour.

The electrochemical parameters obtained by equivalent circuit simulation are shown in Table 3–5. In Table 3, better capacitive behaviour was noticed for the CS/TaN system compared with the uncoated steel. The value of capacitance is related to a degree of reaction from the formation of ionically conducting paths across the coating; coated samples showed a better capacitive behaviour because the R_{pol} values were eight times higher, indicating that the corrosion resistance was improved. In the TS/TaN system (Table 4) the Q_{surf} and R_{pore} values show a drastic positive change, which indicates a higher resistance to electrolyte penetration through pores and also better capacitive behaviour. The coating capacitance is generally considered to provide information about the degree of electrolyte penetration

Table 3 Electrochemical parameters of CS/TaN system obtained by EIS simulation using equivalent circuits

Specimen	Time, h	$Q_{surf}, \mu F cm^{-2}$	n	$R_{pol}, k\Omega cm^2$
CS	1	172.2	0.776	3.9
	24	220	0.749	4.1
	48	207.9	0.748	4.1
	72	215.3	0.739	4.0
CS/TaN	1	38.9	0.719	29.8
	24	60.7	0.761	24.9
	48	65.9	0.777	16.8
	72	61.7	0.795	15.9

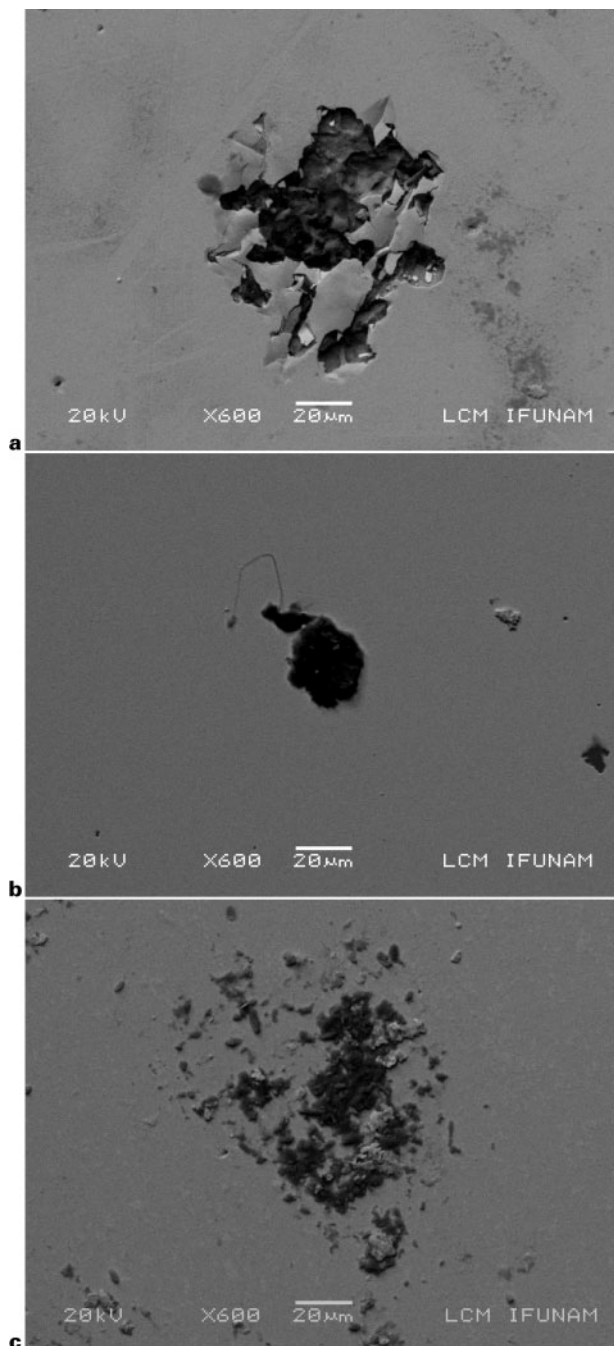
Table 4 Electrochemical parameters of TS/TaN system obtained by EIS simulation using equivalent circuits

Specimen	Time, h	$Q_{surf}, \mu F cm^{-2}$	N	$R_{pore}, \Omega cm^2$	$Q_{dl}, \mu F cm^{-2}$	n	$R_{pol}, k\Omega cm^2$
TS	1	168.9	0.832	48.9	142.3	0.809	5.8
	24	223.4	0.812	61.2	779.1	0.801	4.4
	48	310.2	0.782	59.8	1584	0.881	3.6
	72	412.3	0.729	62.5	2338	0.885	3.0
TS/TaN	1	5.2	0.862	1813	14.5	0.791	73.4
	24	8.3	0.857	815	125.6	0.850	45.1
	48	10.7	0.834	566.2	307.6	0.908	26.5
	72	14.1	0.799	593.4	458.5	0.892	19.4

Q_{dl} : Double layer copacitance.

Table 5 Electrochemical parameters of SS/TaN system obtained by EIS simulation using equivalent circuits

Specimen	Time, h	$Q_{surf}, \mu F cm^{-2}$	n	$R_{pore}, k\Omega cm^2$	$Q_{surf}, \mu F cm^{-2}$	n	$R_{pol}, k\Omega cm^2$	$W_{diffusion}, F cm^{-2}$
SS	1	6	0.837	14.7	59	0.781	130	
	24	11.4	0.859	4.1	17.3	0.868	379	
	48	9.6	0.862	3.8	15.9	0.877	424	
	72	8.4	0.862	3.5	14.8	0.889	473	
SS/TaN	1	7.1	0.888				1319	0.142
	24	7.6	0.876				1409	0.236
	48	7.8	0.875				1234	0.287
	72	7.9	0.852				1119	0.821



a CS/TaN system; b SS/TaN system; c TS/TaN system
9 SEM images of surface films after 72 h of immersion in 3%NaCl

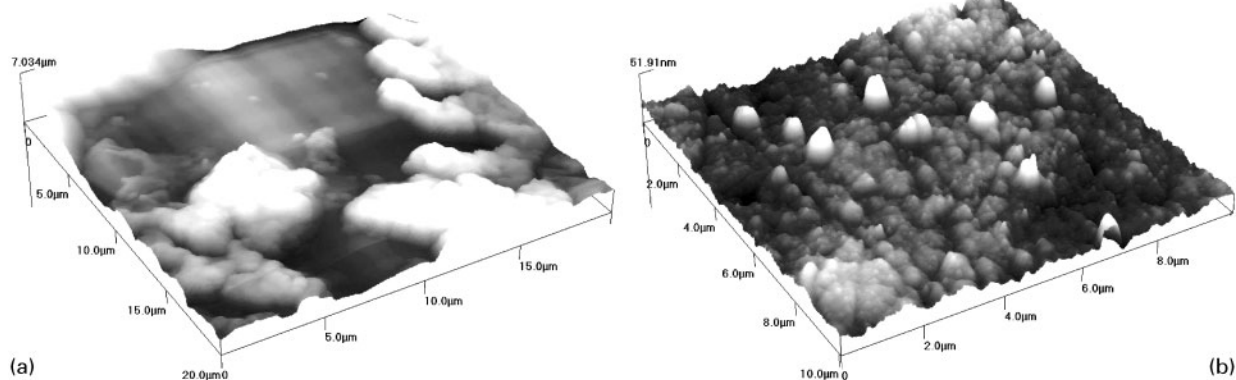
through surface defects and in principle the value is expected to increase with immersion time if a passive film is not formed.²⁸ Finally, Table 5 presents the electrochemical parameters for the SS and SS/TaN systems. The polarisation resistance R_{pol} was ten times higher for the coated metal and a more effective passive film with better dielectric properties was observed.

After the immersion test, the morphology and corrosion features of each coated system were examined by SEM and the resulting micrographs are shown in Fig. 9a–c. Figure 9a shows the results for the CS/TaN system; local delamination of the TaN film owing to the formation and spalling of non protective corrosion products was observed. The surfaces of TS/TaN and SS/TaN samples (Fig. 9b and c) respectively show evidence of less destructive corrosion processes with many corrosion products resulting from the dissolution of the substrate.

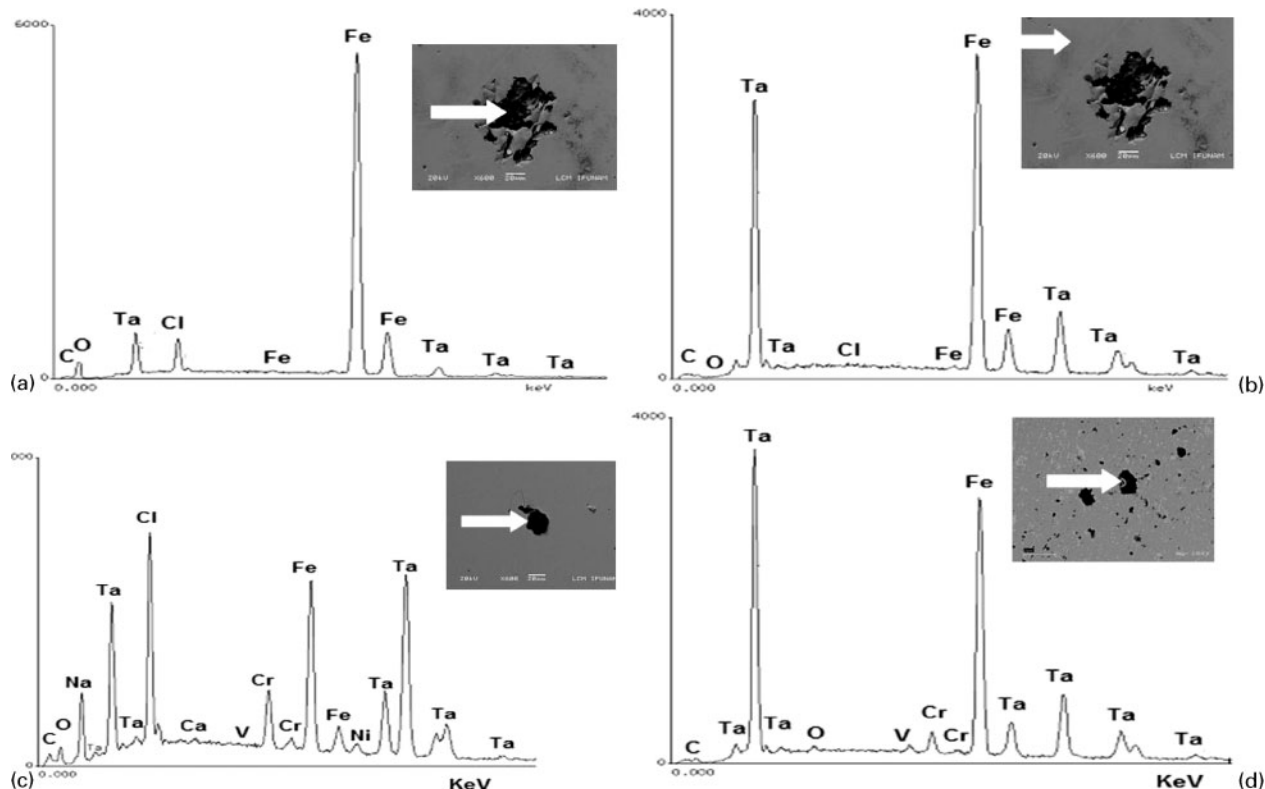
The AFM technique was employed to study the formation of passive films, pits and corrosion products. A significant damage was observed on the CS surface after 72 h of immersion in the solution, a height of 7 µm was observed on the AFM analysis (Fig. 10a) and a general corrosion process was detected. Figure 10b presents the micrograph for the coated steel after the EIS test; the surface damage was significantly less compared with the uncoated steel.

The chemical composition of the corrosion products of the film after 72 h of immersion in the solution was obtained by EDAX analysis. Figure 11a–d shows the qualitative elemental analysis for the different systems. Figure 11a and b shows the analysis for the CS/TaN system; the presence of mineral salts and oxide corrosion products was observed. Iron oxides and hydroxides are not stable protective compounds; their spalling results in film delamination. For the SS/TaN and TS/TaN systems shown in Fig 11c and d respectively, elements like Cr, Ni and V form more protective and passive films. These results are in agreement with the formation of a second time constant and a diffusional process in the EIS analysis.

Figure 12a and b represents the corrosion mechanisms of the CS/TaN and SS/TaN systems respectively. Local defects, such as pinholes, provide direct paths between the corrosive environment and the thin film/substrate. For the CS/TaN system (Fig. 12a), the EIS analysis (Fig. 5a) showed the presence of one relaxation time without the formation of any passive film. The electrolyte easily penetrated into the pores and the



a CS; b CS/TaN system
10 AFM images of uncoated and coated CS steel after 72 h of immersion in 3%NaCl



a delamination area CS/TaN system; b area without delamination CS/TaN system; c SS/TaN system; d TS/TaN system
 11 Chemical analysis by EDAX on system surfaces after 72 h of immersion in 3%NaCl

non-protective corrosion products (Fig. 11b) formed on the steel surface did not provide noticeable resistance to its penetration and the corrosion of the substrate occurred.

For the SS/TaN system (Fig. 12b), the EIS (Fig. 7a) indicated the formation of a dense passive film with high dielectric constants in the pores. In this system, no delamination process was detected (Fig. 9b).

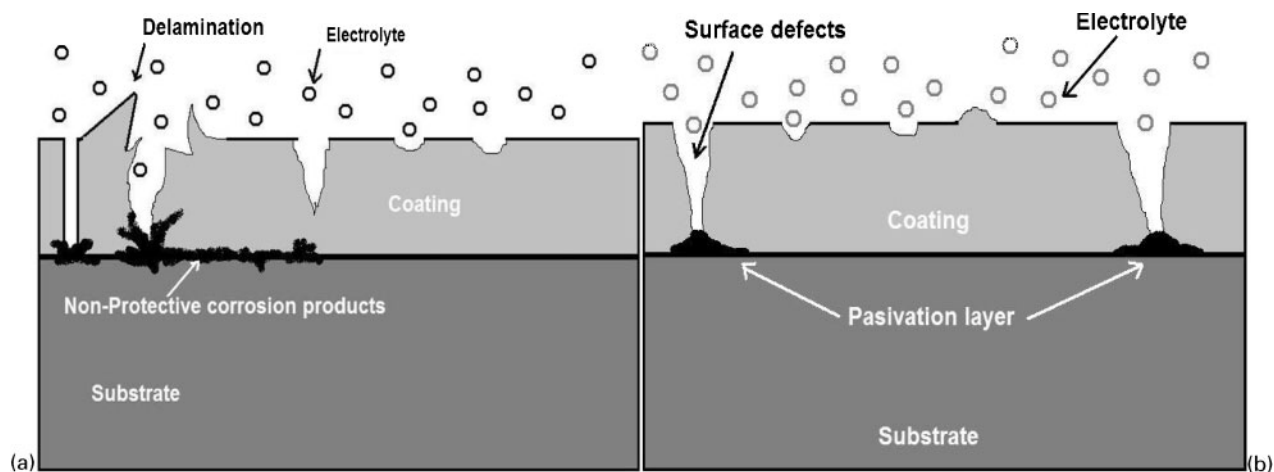
Conclusions

X-ray diffraction patterns have shown that TaN films on a CS of type AISI 1018, a TS of type AISI M2 and an SS of type AISI 304 have a face centred cubic structure, the diffraction planes being {111}, {200} and {220}. The

films have a very fine granular structure with a round shape. The crystalline structure and the surface morphology of the film are not influenced by the substrate.

The polarisation plots of all the coated samples display better corrosion resistance than that of uncoated steels, but the polarisation plots of the systems reproduced some features of the substrates' shape owing to the interconnection of the films and the medium by surface defects such as pores, pinholes and droplets.

A charge transfer process with a relaxation time constant was indicated by EIS for the CS and the CS/TaN system, the coated carbon steel displaying capacitive and resistive behaviour. Two relaxation times were detected for the TS/TaN system, implying that the films contain surface defects. These constitute conductive



a CS/TaN system; b SS/TaN system

12 Corrosion mechanisms of studied systems

paths in the films and allow the penetration of corrosive species which is detrimental to the coated TS. The SS/TaN system displays evidence of a diffusion process, the capacitive behaviour of the passive films indicating a phase angle close to 90°.

Surface analyses (SEM, EDAX and AFM) demonstrated that the corrosion attack on the film surface during immersion in a chloride solution produced a localised form of delamination and pitting attack. For the CS/TaN system, the development of rapid localised corrosion resulted in delamination. The presence of non-protective corrosion products (iron oxides and hydroxides) was detected by EDAX analysis.

A less destructive corrosion process was observed for the SS/TaN and TS/TaN systems. The Cr and O peaks detected in the EDAX spectrum demonstrated the formation of protective passive films.

The thin TaN films demonstrated their capability to improve the corrosion performance of bulk metals. Thin ceramic films are widely employed in the electronics industry. Corrosion protection is important to ensure the reliability of its products.

Acknowledgements

The authors are grateful for the financial support provided by Consejo Nacional de Ciencia y Tecnología (CONACYT). The authors also wish to express the thankfulness for the technical and financial supports to the Universidad Nacional Autónoma de México (UNAM), Universidad Autónoma de Nuevo León (UANL) and Universidad Autónoma de Baja California (UABC).

References

1. P. J. Kelly and R. D. Arnell: *Vacuum*, 2000, **56**, 159–172.
2. K. Baba, R. Hatada, R. Emmerich, B. Enders and G. K. Wolf: *Nucl. Instrum. Method. B*, 1995, **106B**, 106–109.
3. G. F. Huang, L. P. Zhou, W. Q. Huang, L. H. Zhao, S. L. Li and D. Y. Li: *Diam. Relat. Mater.*, 2003, **12**, 1406–1410.
4. H. P. Feng, C. H. Hsu, J. K. Lu and Y. H. Shy: *Mater. Sci. Eng. A*, 2003, **347A**, 123–129.
5. H. B. Nie, S. Y. Xu, S. J. Wang, L. P. You, C. K. Ong, J. Li and T. Y. F. Liew: *Appl. Phys. A*, 2001, **73A**, 229–236.
6. W. H. Lee, J. C. Lin and C. Lee: *Mater. Chem. Phys.*, 2001, **68**, 266–271.
7. H. Kawasaki, K. Doi, J. Namba and Y. Suda: *Mater. Res. Soc. Symp.*, 2000, **617**, J3-22-1–J3-22-5.
8. S. Tsukimoto, M. Moriyama and M. Murukami: *Thin Solid Films*, 2004, **460**, 222–226.
9. L. Shi, Z. H. Yang, L. Y. Chen and Y. T. Qian: *Solid State Commun.*, 2005, **133**, 117–120.
10. L. Gladczuk, A. Patel, J. D. Demaree and M. Sosnowski: *Thin Solid Films*, 2005, **476**, 295–302.
11. K. Baba, R. Hatada, K. Udoh and K. Yasuda: *Nucl. Instrum. Method. B*, 1997, **127B**, 841–845.
12. K. Baba and R. Hatada: *Surf. Coat. Technol.*, 1996, **84**, 429–433.
13. D. Y. Zhang, Q. Lin, Q. Y. Fei, H. M. Zhao, G. Y. Kang and M. Geng: *Rare Met.*, 2003, **22**, 276–279.
14. W. C. Mack (ed): 'Worldwide guide to equivalent irons and steels', 4th edn; 2000, Materials Park, OH, ASM International
15. Y. Y. Lee, C. Heck, S. Y. Chun, A. Chayahara, Y. Horino, W. Ensinger and B. Enders: *Surf. Coat. Technol.*, 2002, **158–159**, 588–593.
16. A. Zeng, E. Liu, I. F. Annergren, S. N. Tan, S. Zhang, P. Hing and J. Gao: *Diam. Relat. Mater.*, 2002, **11**, 160–168.
17. D. K. Merl, P. Panjan, M. Cekada and M. Macek: *Electrochimica Acta*, 2004, **49**, 1527–1533.
18. S. M. Meang: 'Corrosion studies on tantalum and tantalum coated steel', PhD thesis, New Jersey Institute of Technology, Newark, NJ, USA, 2005.
19. S. H. Ahn, J. H. Lee, J. G. Kim and J. G. Han: *Surf. Coat. Technol.*, 2004, **177–178**, 638–644.
20. A. Zeng, E. Liu, S. N. Tan, S. Zhang and J. Gao: *Electroanalysis*, 2002, **14**, 1110–1115.
21. R. D. Mansano, M. Massi, A. P. Mousinho, L. S. Zambom and L. G. Neto: *Diam. Relat. Mater.*, 2003, **12**, 749–752.
22. M. Lakatos-Varsanyi and D. Hanzel: *Corros. Sci.*, 1999, **41**, 1585–1598.
23. M. Khaled, B. S. Yilbas and J. Shirokoff: *Surf. Coat. Technol.*, 2001, **148**, 46–54.
24. I. Milosev and B. Navinsek: *Surf. Coat. Technol.*, 1994, **63**, 173–180.
25. A. Vijayakumar, T. Du, K. B. Sundaram and V. Desai: *Microelectron. Eng.*, 2003, **70**, 93–101.
26. S. H. Ahn, Y. S. Choi, J. G. Kim and J. G. Han: *Surf. Coat. Technol.*, 2002, **150**, 319–326.
27. C. Liu, Q. Bi, A. Leyland and A. Matthews: *Corros. Sci.*, 2003, **45**, 1243–1256.
28. J. H. Yoo, S. H. Anh, J. G. Kim and S. Y. Lee: *Surf. Coat. Technol.*, 2002, **157**, 47–54.
29. C. Liu, Q. Bi, A. Leyland and A. Matthews: *Corros. Sci.*, 2003, **45**, 1257–1273.

Copyright of Corrosion Engineering, Science & Technology is the property of Maney Publishing and its content may not be copied or emailed to multiple sites or posted to a listserv without the copyright holder's express written permission. However, users may print, download, or email articles for individual use.